COMPARATIVE STUDY OF DIFFERENT DYNAMIC STRENGTH MODELS IN SIMULATING IMPACT-DRIVEN SPALLATION

V.R.Ikkurthi, S.Chaturvedi
Computational Analysis Division, Bhabha Atomic Research Centre, Visakhapatnam, INDIA-500012
E-mail of corresponding author: ramana468@gmail.com

ABSTRACT

Computer simulations are necessary to evaluate the behavior of reactor structures under accident situations, such as the production of pulsed high pressures in pressure vessels or containment structures. The response of the structure to such pulses depends critically upon the dynamic strength of the structure material, i.e., the variation of elastic moduli and yield strength with strain, strain rate, pressure, temperature, etc. A variety of dynamic strength models are available in the literature. It is necessary to evaluate their relative performance through laboratory experiments and simulations. The aim of the present paper is a comparative study of various dynamic strength models for the specific case of impact-driven spallation in metals. Our results for the spall strength, computed using the Steinberg-Guinan (SG) and Zerilli-Armstrong (ZA) strength models, agree reasonably well with experimental values from a Russian spall database. The Revised Johnson-Cook model generally does not agree well with experimental results. The ZA model shows the best overall agreement, in terms of both spall strength and spall thickness, especially when the spall thickness computation is based upon the void volume fraction.

INTRODUCTION

Reactor structures can be subjected to different accident situations, such as the production of pulsed high pressures in pressure vessels or containment structures. The response of the structure to such loads depends critically upon the dynamic strength of the structure material, i.e., the variation of elastic moduli and yield strength with strain, strain rate, pressure, temperature, etc. The structure can even spall or fracture. Computer simulations are necessary to evaluate such phenomena.

"Spall fracture"' is damage that occurs in a body when two rarefaction waves interact and produce enough dynamic tension to fracture it. Physically, spall fracture occurs simultaneously over an area by the nucleation, growth and coalescence of many micro cracks or voids. Consider the case of flyer-target impact problem, where the diameters of both the flyer and the target are much greater than their thicknesses. In such a case, planar impact generates two one-dimensional shock waves. One propagates into the target and the other into the metal plate. These shock waves reflect as rarefaction waves from the free surfaces of the flyer and target plates respectively. With a thin flyer, these rarefaction waves interact inside the target, producing a state of tension in some region. If this tensile stress level exceeds the dynamic yield strength of the material, fracture takes place, producing a scab ("spall element"') from that section of the target. After fracture has taken place, stress or spall signals are produced that propagate to, and accelerate, the free surface of the target [1]. The velocity and the thickness (``spall thickness") of this scab depends upon the shape of the pressure profile at the free surface and the yield strength of the target.

A large set of spall experiments have been carried out by Kanel and co-workers, and the results compiled [2]. These experiments include measurement of the time-dependent free-surface velocity of the spall element, from which one can calculate the spall strength of the material and the thickness of the spall element. Here, "spall strength"' refers to the relative resistance of the material to spallation.

We have been carrying out a systematic programme of one-dimensional (1-D) and two-dimensional (2-D) hydrodynamic simulations, using an Arbitrary-Lagrangian-Eulerian (ALE) code [1, 3] to study spallation in impact-loaded copper and mild steel (MS) plates. We have implemented various Equation of State (EOS) models, four damage models and three material dynamic strength models in the code.

In our previous work [1], the spall parameters obtained from simulations were compared with a set of Russian spall experiments [2]. We compared the ability of four damage models to reproduce experimental results. The damage models incorporated included the Void-Growth (VG) model, Nucleation and Growth (NAG) model, Johnson-Cook (JC) model and Cochran-Banner (CB) model [1]. Our simulations showed that the VG and DFRACT models yielded spall parameters that agreed reasonably well with experiments, with VG yielding the best match. In that work, we also reported the results of simulations to study the effect of parameters like impact pressure, tensile wave duration and initial target temperature on spall parameters [1].

Spallation is a rate-dependent phenomenon, in which voids nucleate, grow and coalesce depending upon the loading conditions. When a material is dynamically loaded, its temperature and strength varies. The hydrodynamic codes used to simulate such experiments should incorporate material dynamic strength models, to compute the varying strength of the material. Hence these models play a very important role in simulating spall fracture. There exist many computational dynamic strength models developed over years. Before using any model for a practical application, it is necessary to perform a comparative study of these models to find their efficiency in predicting spall fracture. This is the topic of the present work.

For the present work, we have implemented three material strength models in the ALE code. These include the Steinberg-Guinan (SG) strain-rate independent model [4], the Zerilli-Armstrong (ZA) model [5] and the Revised Johnson-Cook (RJC) model [6]. We have performed 1-D simulations to study the effect of these models on the spallation phenomenon.

DESCRIPTION OF DYNAMIC STRENGTH MODELS

A dynamic strength model for a material computes the dynamic strength of the material in terms of the Yield strength (Y) and Shear modulus (G), which are given as functions of the temperature (T), strain (ε), strain rate ($\dot{\varepsilon}$) and Pressure (P). The first three variations are referred to as thermal softening, work hardening and strain-rate hardening, respectively. Many strength models, both empirical and micro-structural in nature, have been developed to describe dynamic strength of materials. These include the Steinberg-Guinan (SG) strain-rate-independent model [4], Zerilli-Armstrong (ZA) [5], Revised Johnson-Cook (RJC) [6], Bodner-Partom (BP) [7], Mechanical Threshold Stress (MTS) [8] and the Steinberg-Guinan (SG2) strain-rate-dependent model [9]. Each model includes certain coefficients which must be obtained as best-fit values for each material.

In the present work, our objective is to compare theoretical predictions using different strength models with certain spall experiments [2], to study the effectiveness of strength models in predicting spall. We have carried out 1-D simulations with the SG, ZA and RJC models. The study has been restricted to these models because model coefficients are available for the materials of interest, viz. copper (Cu) and mild steel (MS). These models are explained in following subsections. The other models require coefficients that are not available for Cu and MS. For these models, a systematic optimization study is required to determine best-fit model coefficients for Cu and MS, by matching against experimental results. Such a study lies beyond the scope of the present work. However, it is planned in the future.

Steinberg-Guinan Strain-rate Independent Strength Model

The Steinberg-Guinan (SG) model [4] accounts for the effects of pressure (P), temperature (T) and equivalent plastic strain (ε_p) on Y and G. The model assumes a minimal effect of strain rate ($\dot{\varepsilon}$) on Y and is termed as strain rate independent model. Hence, this model is applicable only at high strain rates ($\geq 10^5$ s^{-1}). The strength equations for Y and G in the SG model are:

$$Y = Y_{pl}\left[1+\left(\frac{Y_p^{'}}{Y_0}\right)\frac{P}{\eta^{1/3}}+\left(\frac{Y_T^{'}}{Y_0}\right)(T-300)\right]$$

$$G = G_0\left[1+\left(\frac{G_p^{'}}{G_0}\right)\frac{P}{\eta^{1/3}}+\left(\frac{G_T^{'}}{G_0}\right)(T-300)\right]$$

where

$$Y_{pl} = Y_0\left[1+\beta\left(\varepsilon_p+\varepsilon_i\right)\right]^n$$

represents the strain hardening term, and is subjected to the limitation that $Y_{pl} \leq Y_{\max}$.

Here, η is the compression, i.e., the ratio of initial and current specific volumes. β and *n* are work-hardening parameters. ε_i is the initial equivalent plastic strain, which is normally adjusted so as to reproduce the measured initial yield strength. The subscript '0' refers to the reference state (T = 300 K, P = 0, ε = 0). $G_T^{'}$ and $G_P^{'}$ are the rates of change of shear modulus with temperature and pressure, respectively. $Y_T^{'}$ and $Y_p^{'}$ are defined in the same way. The model coefficients for the materials of interest, viz., Cu and MS, have been taken from [4].

Zerilli-Armstrong Strength Model

Many strength models, such as the SG and JC models, are empirical in nature. These are essentially numerical fits to test data and their validity outside the limited range of the test data is doubtful. Also, these models do not account for the grain size of the structure, though it is known that this can have a dramatic effect on the strength and ductility of materials.

The Zerilli-Armstrong (ZA) model [5] is based on the framework of thermally activated dislocation motion. The model consists of two micro-structurally based constitutive equations to predict the dynamic strength of two different crystalline structures, viz., body-centered cubic (bcc) and face-centered cubic (fcc). The formulation of the model is as follows:

For fcc crystals:

$$Y = \Delta\sigma_G^{'} + C_2\varepsilon^{1/2}\exp\left(-C_3T + C_4T\ln\dot{\varepsilon}\right) + kl^{-1/2}$$

For bcc crystals:

$$Y = \Delta\sigma_G^{'} + C_1\exp\left(-C_3T + C_4T\ln\dot{\varepsilon}\right) + C_5\varepsilon^n + kl^{-1/2}$$

Here, the $C_i^{'}$s and *n* are model coefficients. The first term, $\Delta\sigma_G^{'}$, accounts for the influence of solutes and the original dislocation density on the yield stress [5]. The last term in both equations is the product of a micro-structural stress intensity (*k*) and the inverse square root of the average grain diameter (*l*). The exponential term in both equations is responsible for the thermal activation.

Two points are noteworthy. Firstly, the ZA model does not contain the effect of hydrodynamic pressure on Y. Secondly, it does not indicate anything about the variation of the shear modulus G. Hence we have used the same form for variation of G as that proposed in the SG model. The material coefficients and exponents for Cu and MS have been taken from [5].

Revised Johnson-Cook Strength Model

The Johnson-Cook (JC) material model [10] has an empirical basis. It expresses the flow stress as a function of plastic strain, strain rate and temperature. The model [10] was first proposed in 1983 and has the following form:

$$Y = \left(C_1 + C_2\varepsilon^n\right)\left(1 + C_3\ln\dot{\varepsilon}^*\right)\left(1 - T^{*m}\right)$$

where the $C_i^{'}$s, *m* and *n* are model coefficients. $\dot{\varepsilon}^*$ is the dimensionless equivalent plastic strain rate, given by $\dot{\varepsilon}^* = \dot{\varepsilon}/\dot{\varepsilon}_0$, with $\dot{\varepsilon}_0 = 1.0$. T^* is the homologous temperature, given by $T^* = \dfrac{T - T_{room}}{T_{melt} - T_{room}}$.

The JC model uses simple scalar expressions to represent the strains and strain rates, which are actually second-order tensors. It has been found that, for many ductile materials, the yield strength increases more rapidly with strain rate than that predicted by the JC model, for strain rates in excess of 10^3 s^{-1} [11]. In order to increase the strain-rate sensitivity, a modified Johnson-Cook (MJC) strength model was proposed in 1991 [11]. This has the following form:

$$Y = \left(C_1 + C_2\varepsilon^n\right)\left(\dot{\varepsilon}^{*\chi}\right)\left(1 - T^{*m}\right)$$

where χ is an empirical exponent. However, the MJC strength model is not widely used today, probably because the strain rate sensitivity is not significantly improved over that provided by the JC model.

To account for the rapid increase of *Y* with $\dot{\varepsilon}$, the revised Johnson-Cook (RJC) strength model [6] was proposed in 1998. This model has the following form for dynamic strength:

$$Y = \left(C_1 + C_2\varepsilon^n\right)\left(1 + C_3\ln\dot{\varepsilon}^* + C_4\left[\frac{1}{C_5 - \ln\dot{\varepsilon}^*} - \frac{1}{C_5}\right]\right)\left(1 - T^{*m}\right)$$

where C_4 and C_5 are additional empirical coefficients. C_4 controls the amount of deviation of the strain rate behavior as compared to the JC model. C_5 is the natural logarithm of a critical strain rate level [6]. The strain rate sensitivity has been enhanced by the term $\dfrac{1}{C_5 - \ln\dot{\varepsilon}^*}$. This term tends to infinity as the strain rate approaches the critical value, resulting in a physically untenable infinite yield strength. To prevent this unrealistic occurrence, the RJC

model assumes that there exists a maximum value that the strain rate sensitivity factor can attain for each material. This peak value cannot be exceeded regardless of the prevailing strain and temperature state. The peak strain rate sensitivity factor is defined through the non-dimensional constant C_6 as follows [6]:

$$\left(1 + C_3 \ln \dot{\varepsilon}^* + C_4 \left[\frac{1}{C_5 - \ln \dot{\varepsilon}^*} - \frac{1}{C_5} \right] \right) \leq C_6$$

The entire strain rate sensitivity enhancement term is set to zero for strain rates of less than unit magnitude. A few points need to be noted regarding the RJC model. Firstly, the model does not include the variation of Y with hydrodynamic pressure P. Secondly, due to the correction term $-1/C_5$, the strain rate sensitivity enhancement contribution tends toward zero for low strain rates. Thus the RJC model approaches the original JC model for low strain rates and is identical to the JC model at a strain rate of unit magnitude. So, the RJC model is identical to JC model for $\dot{\varepsilon}$ values of unity or less. The RJC model coefficients for Cu and MS have been taken from [6].

DESCRIPTION OF METHODOLOGY

Simulations have been performed for some of the experiments described in a compilation of Russian spall data [2]. Details of the experiments are given in Table.1.

The ALE code is capable of handling 2-D geometries. However, 1-D simulations are sufficient to perform a comparative study of material dynamic strength models. The methodology of simulation is basically the same as that described in [1]. Hence only the salient features are described here. The simulation starts at the moment of impact. A schematic of the computational domain for one-dimensional (1-D) simulations is shown in Fig.1, along with boundary conditions. We have used the HOM EOS for Aluminum [12] and a six-parameter EOS for Copper and Mild Steel (MS) [1, 13].

Table 1. Description of spall experiments simulated [2]. Material densities of Al, Cu and Mild Steel used in the simulations are 2785, 8930 and 7860 kg/m^3 respectively.

Expt. Label	Flyer Plate				Target Plate		
	Material	Thickness (cm)	Diameter (cm)	Velocity (m/sec)	Material	Thickness (cm)	Diameter (cm)
B16	Al	0.2	12	660	MS	1.0	12
B61	Al	0.2	12	450	Cu	1.5	12
B62	Al	0.2	12	450	Cu	1.2	12
B63	Al	0.02	1.2	660	Cu	0.39	1.2
B65	Al	0.04	1.2	660	Cu	0.27	1.2

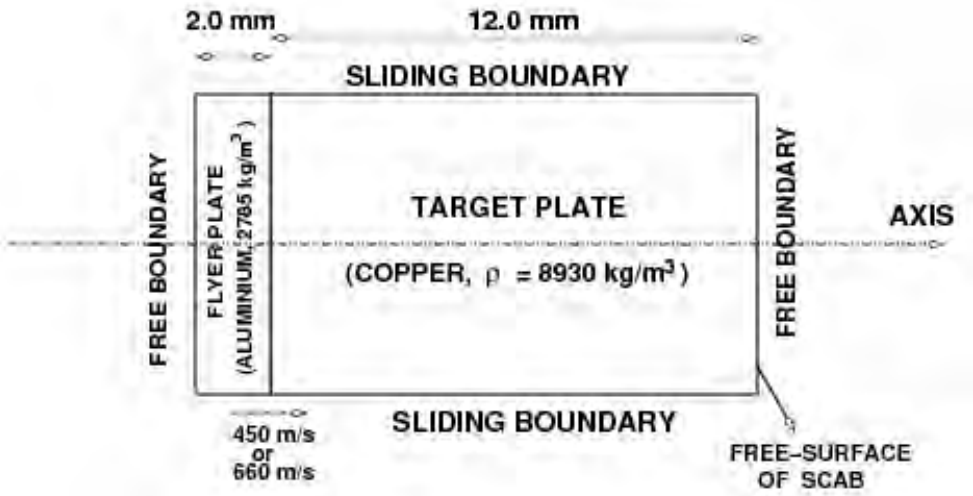

Fig.1: Schematic of the computational mesh for 1-D simulation (not to scale). Boundary conditions are also specified. The thicknesses of both plates are greatly exaggerated.

Details of fracture model

Our earlier work [1] had shown that the Void Growth (VG) model yields the best match with experimental results. Hence, in the present work, we have only used the VG fracture model. Details of four fracture models are given in Ref.[1]. For the sake of completeness, however, the VG model is summarized below.

In this model, the presence of voids in each computational cell is expressed in terms of the distension ratio α, which is related to the porosity φ through the expression φ = 1 – 1/α. The rate of change of α is given by

$$\dot{\alpha} = 0, \Delta p \geq 0$$

$$\dot{\alpha} = -\frac{(\alpha - 1)^{2/3}}{\eta}\alpha(\alpha - 1)^{1/3}\Delta p, \Delta p < 0$$

where Δp is the driving stress for void growth, given by

$$\Delta p = \bar{p} + \frac{a_s}{\alpha}\ln\left(\frac{\alpha}{\alpha - 1}\right)$$

Here η is a material parameter with units of (stress × time). a_s having units of stress, represents the threshold for void growth. The parameter a_0 provides the initial distension to get the void-growth process started. The variable $\bar{p}$ is the average mean stress in the porous region containing voids. The VG model constants used in the simulations for Cu and MS materials have been taken from [1].

Calculation of Spall Parameters

We monitor the temporal variation of the free-surface velocity, $v_{fs}(t)$, of the spalled element and the spatio-temporal evolution of the void volume fraction (VVF), viz. φ in the VG model, within the target. If spallation takes place, a pull-back occurs in the free-surface velocity profile. The stress waves propagate back and forth in the spalled element, producing oscillations in the free-surface velocity profile.

We use three methods to compute the spall parameters, viz., spall strength (P_{sp}) and spall element thickness (t_s). The first method is to use the Pull-back Velocity (Δw) and the period (T_p) of the oscillations, both obtained from the free-surface velocity profile. The following equations [1] are used to compute P_{sp} and t_s.

$$P_{sp} = \frac{1}{2}\rho_0 C_b \Delta w$$
$$t_s = \frac{1}{2}C_b T_p \qquad (1)$$

where ρ_0 and C_b are density and bulk sound speed at zero pressure.

The second method is based on VVF evolution [1]. We assume that when VVF in a computational cell approaches a critical value of 0.3, spallation takes place at that point. The spall thickness can then be calculated as the distance from that cell to the free surface. As VVF grows in a material, the material gets softened and its strength degrades. The third method of calculating spall parameters is to identify the computational cell where the shear modulus drops to half its normal value and spall thickness would be the distance from that cell to the free surface. The justification for using the last two criteria is given in Ref.[1].

RESULTS

Free-surface velocity

As mentioned in the previous sections, 1-D simulations are sufficient for developing insight into the spallation process, and for determining spall parameters like spall strength and spall thickness. We have performed such simulations for the experimental configurations listed in Table.4 by varying the strength models.

Figure 2 shows the computed free-surface velocity profiles of the spalled element in a mild steel target, using 1-D simulations with the SG, ZA and RJC material strength models. This has been done for the parameters of the experiment labeled B-16 in Table.1. The experimental free-surface velocity profile published in the Russian Spall database is also shown for comparison. There is considerable difference between the experimental and computed profiles, regardless of the model used.

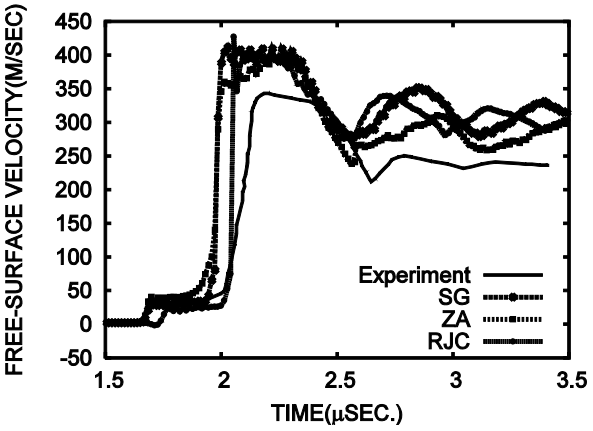

Fig.2: Experimental and computed free-surface velocity profiles for experiment labeled B-16 using SG, ZA and RJC models, with a mild steel target.

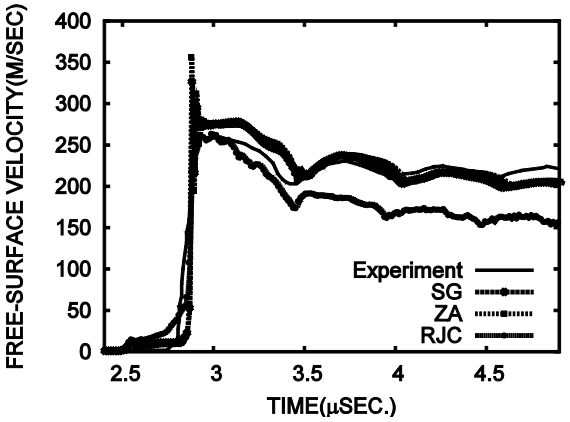

Fig.3: Experimental and computed free-surface velocity profiles for experiment labeled B-62 using SG, ZA and RJC models, with a copper target.

Figure 3 shows the same plots for a copper target, corresponding to the B62 experiment in Table.1. We see that the SG and ZA models yield similar velocity profiles, which match reasonably well with the experimental profile. Fig.4 shows the results for the B65 experiment. All models now deviate considerably from the experimental profile. The SG and ZA curves are similar. Also, we observe that the pull-back (spall signal) in velocity starts at slightly higher velocities when we use SG and ZA models, as compared to that obtained with the RJC model. This implies a smaller value of spall strength, as can be seen from Equation (1).

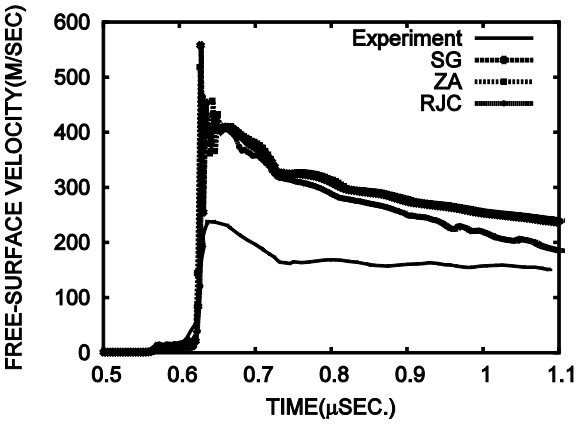

Fig.4: E experimental and computed free-surface velocity profiles for experiment labeled B-65 using SG, ZA and RJC models, with a copper target.

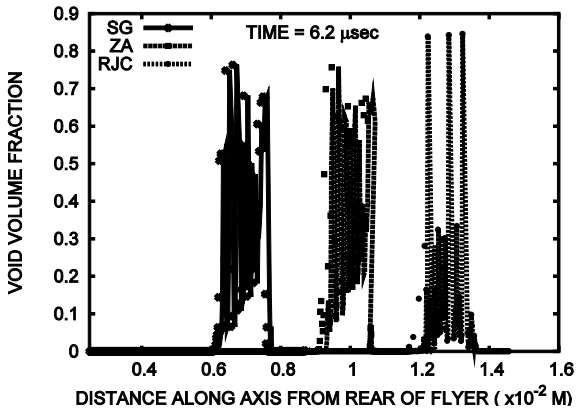

Fig.5: Normalized void volume computed in copper for experiment labeled B-62, using SG, ZA and RJC models. The curves corresponding to different models have been displaced for clarity; otherwise, void growth occurs in the same region with all models.

Figure 5 shows the computed VVF in the copper target, for the B62 experiment. The curves computed using the three models have been displaced for greater clarity; otherwise, VVF growth occurs in the same region, as is only to be expected. The SG and ZA results are broadly similar, while RJC is qualitatively different. Fig.6 shows the computed spall strength values for various experiments.

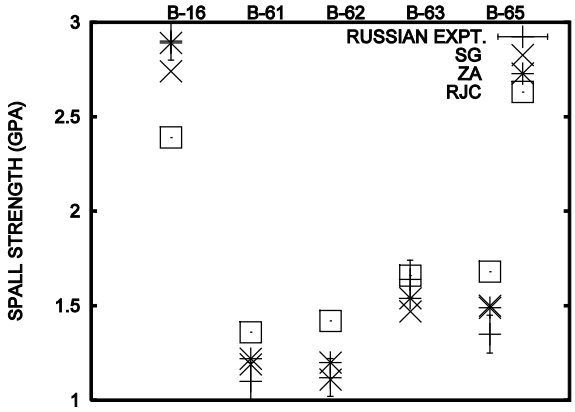

Fig.6: Computed spall strength values for various experiments

Table 2. Computed P_{sp} values using SG, ZA and RJC models (1-D simulation)

Expt. label	Russian Expt. (± 0.1 GPa)	SG (GPa)	ZA (GPa)	RJC (GPa)
B16	2.9	2.74	2.89	2.39
B61	1.1	1.19	1.22	1.36
B62	1.12	1.11	1.2	1.42
B63	1.64	1.47	1.54	1.66
B65	1.35	1.5	1.49	1.68

Discussion

The computed P_{sp} and t_s values for different experiments are summarized in Tables 2 and 3, respectively. In Table.3, t_{s1} and t_{s2} refer to the spall thicknesses calculated using $v_{fs}(t)$ and the VVF, respectively. The VVF and shear modulus criteria, explained in previous section, yield essentially the same t_s, hence only the VVF value is shown in Table.3. For some cases, where blanks appear in Table.3, the simulations did not yield well-defined spall signals, hence spall thickness calculations were not performed.

From Table.2, for all experiments involving copper targets, we observe that the RJC model yields larger P_{sp} values as compared to the ZA model, which in turn yields larger values than the SG model. The sole exception is B65, where the ZA and SG values are almost identical. Also, for all experiments, the SG and ZA values are generally closer to experimental values, with the exception of B63. Note that the ZA result lies almost within the experimental error (± 0.1 GPa) for all experiments. Hence we conclude that, as far as spall strength is concerned, the ZA model has the best performance for the experiments examined in this study, with SG also doing fairly well. The RJC model generally does not yield a good match.

Table 3. Computed t_s values using SG, ZA and RJC models (1-D simulation)

Expt. label	Russian Expt. (± 10% mm)	SG		ZA		RJC	
		t_{s1} (mm)	t_{s2} (mm)	t_{s1} (mm)	t_{s2} (mm)	t_{s1} (mm)	t_{s2} (mm)
B16	1.16	1.24	1.35	1.29	1.81	1.02	1.15
B61	1.24	1.03	1.09	1.11	1.13	0.93	1.15
B62	1.15	1.1	0.9	1.09	1.2	1.07	1.34
B63	0.18	-	0.13	-	0.23	0.15	-
B65	0.23	0.18	0.18	0.18	0.24	0.16	0.26

The following points can be noted from Table.3. Firstly, the t_s values obtained using the VVF criterion (t_{s2}) are generally larger than the values obtained from free-surface velocity profiles (t_{s1}). The only exceptions are the B62 and B65 experiments when the SG model is used. Secondly, the ZA model yields larger t_{s1} values than RJC. Thirdly t_{s2} computed using the ZA model lies within the experimental error for three experiments, viz., B61, B62 and B65. For the other two experiments, however, it deviates significantly from experiment.

The overall conclusion is that the ZA model generally yields the best match with experimental results. Both SG and ZA models yield a reasonable match with experiments, with the ZA model yielding spall strength values that generally lies within experimental error. This could be because the ZA model is a micro-structural model and takes into consideration the crystal structure.

Overall, the RJC model does not perform well for spallation simulations. The reason for the mismatch may be that the coefficients mentioned in Ref. [6] are not appropriate for the materials used in these experiments. It would be interesting to determine best-fit values of RJC model parameters that reproduce this experimental data, but that lies beyond the scope of the present work.

CONCLUSIONS AND FUTURE WORK

Spallation is a phenomenon that could play a role during reactor accidents. The structure response depends significantly upon dynamic strength of the structure material. 1-D simulations have been performed to study the relative performance of three material dynamic strength models, viz., Steinberg-Guinan, Zerilli-Armstrong and Revised Johnson-Cook models. The Void Growth model has been used to determine the spatio-temporal evolution of void volume, taking into account the effect of damage on the material strength and the equation of state.

Spall parameters, such as the spall strength and spall element thickness, have been calculated in two different ways, based upon the free-surface velocity profiles and the distribution of void volume, respectively. Our simulation results for the spall strength, using the SG and ZA models, agree reasonably well with experimental values from a Russian spall database. The RJC model generally does not agree well with experimental results. The ZA model shows the best overall agreement, in terms of both spall strength and spall thickness, especially when the spall thickness computation is based upon the void volume fraction. The SG model, too, generally shows reasonable agreement, although not as good as that with ZA. The ZA model may be performing better because it is a micro-structure based model.

In the future, we plan to extend this study in three directions. The first is the use of strength models other than those that have been examined here, such as the Bodner-Partom and MTS models. The second is a systematic study to determine best-fit coefficients of the RJC model for copper and MS used in the Russian experiments. The third is a study of the role of edge effects on spall element separation.

REFERENCES

[1] Ikkurthi, V.R., Chaturvedi, S., "Use of different damage models for simulating impact-driven spallation in metal plates", *International Journal of Impact Engineering* Vol. 30, 2004, pp. 275-301.

[2] Antoun, T.H., Seaman, L., Curran, D.R., "Dynamic Failure of materials, Volume 2-Compilation of Russian Spall Data", *Technical report No.DSWA-TR-96-77-V2*, Defence Special Weapons Agency, Alexandria, VA, 1998.

[3] Demuth, R.B., Margolin, L.G., Nichols. B.D., Adams, T.F., Smith, B.W., "SHALE: A Computer Program for Solid Dynamics", *Report No. LA-10236*, Los Alamos National Laboratory, 1985.

[4] Steinberg, D.J., Cochran, S.G., Guinan, M.W., "A constitutive model for metals applicable at high-strain rate", *Journal of Applied Physics*, Vol. 51(3), 1980, pp. 1498-1504.

[5] Zerilli, F.J., Armstrong, R.W., "Dislocation-mechanics-based constitutive relations for material dynamics calculations", *Journal of Applied Physics*, Vol. 61(5), 1987, pp. 1816-1825.

[6] Rule, W.K., Jones, S.E., "A revised form for the Johnson-Cook strength model", *International Journal of Impact Engineering*, Vol. 21(8), 1998, pp. 609-624.

[7] Bodner, S.R., Partom, Y., "Constitutive equations for elastic-viscoplastic strain-hardening materials", *Journal of Applied Mechanics*, Vol. 42, 1975, pp. 385-389.

[8] Follansbee, P.S., Kocks, U.F., "A constitutive description of the deformation of copper based on the use of Mechanical Threshold Stress as an Internal State Variable", *Acta Metall*., Vol. 36(1), 1988, pp. 81-93.

[9] Steinberg, D.J., Lund, C.M., "A constitutive model for strain rates from 10^{-4} to 10^{+6} s^{-1}", *Journal of Applied Physics*, Vol. 65(4), 1989, pp. 1528-1533.

[10] Johnson, G.R., Cook, W.H., "A constitutive model and data for metals subjected to large strains, high strain rates and high temperatures", *Proceedings of the Seventh International Symposium on Ballistics*, 1983, pp. 541-551.

[11] Holmquist, T.J., Johnson, G.R., "Determination of constants and comparison of results for various constitutive models", *J. Phys. 1 Colloq. C3 (DYMAT)*, 1991, pp. 853-860.

[12] Mader, C., "Numerical Modeling of Detonations", University of California Press, 1979.

[13] Eliezer, S., Ghatak, A., Hora, H., Teller, E., "An introduction to equations of state, Theory and applications", Cambridge University Press, 1986.